

MATRIX SENSOR FOR SOLAR TRACKING SYSTEMS

Alin Argeseanu,

University Politehnica, Department of MAUE, Timisoara, Romania

Krisztina Leban, Ileana Torac

Institute of Energy Technology, Aalborg University, Aalborg, Denmark

Romanian Academy Timisoara Branch, Timisoara, Romania

Abstract: This paper proposes a novel sensor for solar tracking systems. The new sensor gives good readings regardless of the aging factor of the photosensitive elements. In addition, an overall simplified control of the tracking system is obtained.

Key words: solar tracking, optimal position, matrix sensor, photo resistor.

1. Introduction

In recent years, fuel price and pollution factors determined a growing interest towards renewable energy sources. These green energy sources (wind, solar, biofuell, hydrogen, etc) are exploitable with respect to actual technologies, local and geographical resources. Climate changes in Romania and the prognoses make certain regions optimal for solar energy systems (thermo and photovoltaic) [1]. In Fig.1 the evolution of the average temperature of the ground level (T_{med}) and 100 cm depth (T_{100}) on the period 1964-1999 can be viewed [2].

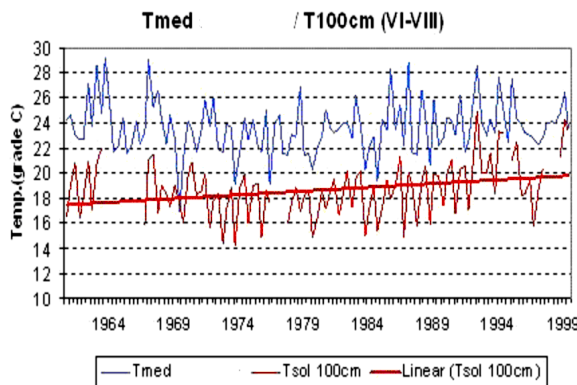


Fig.1. The average temperature evolution

To get maximum efficiency from the solar system, two main solutions are used [3],[4]:

- **Tracking system** implies the mechanical orientation of the solar receiver in order to get the maximum irradiance. With this, efficiency improves by 40%-50% (E-W tracking: 35%-42%; N-S: 5%-8%)

- **Maximum Power Point Tracking System (MPPT)**-traces the point on the PV and IV curves of the solar panels that give the maximum power. Functioning of the panels is held in this point.

The double movement of the Earth imposes the need for solar tracking systems: around the sun and the rotate about its polar axis. Figure 2 shows the Earth's movement and the inclined polar axis.

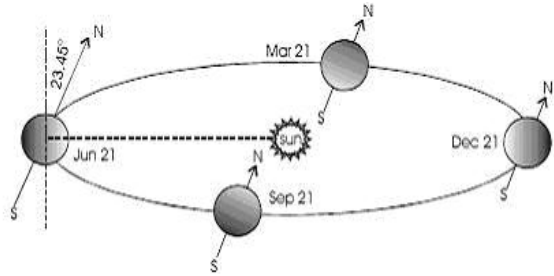


Fig.2. The Earth's orbit

The angle of deviation of the sun from directly above the equator is the declination δ . The expression of the declination in accord with the any given day of the year (n) is:

$$\theta_z = 23.45^\circ \cdot \sin \left[\frac{360 \cdot (n - 180)}{365} \right] \quad (1)$$

The angles north of the equator are considered positive and the angles south of the equator are considered negative.

The zenith angle θ_z is the angle between the sun and the zenith is a line perpendicular to the Earth. Since the solar is directly overhead on the first day of summer at solar noon on the Tropic of cancer, the zenith angle is:

$$\theta_z = \phi - \delta \quad (2)$$

where: ϕ = the latitude (the angular distance from the equator)

The direct normal solar irradiance is:

$$I_{t,h} = I_{b,n} \cdot \cos \theta_z + I_{d,h} \quad (3)$$

where:

$I_{b,n}$ = the irradiance coming directly from the sun
 $I_{d,n}$ = the diffuse radiation

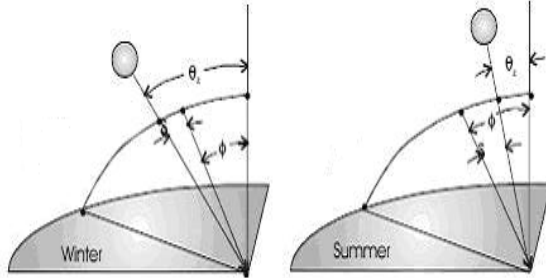


Fig.3. The zenith angle θ_z

The clear-day model of direct normal solar irradiance using the 1962 U.S. Standard Atmosphere (Hottel model) is[3]:

$$I_{b,n} = I_0 \left(a_0 + a_1 e^{-k \frac{1}{\cos \theta_z}} \right) \quad (4)$$

where:

I_0 = the extraterrestrial radiation

a_a, a_1, k = parameters

$$a_a = 0.4237 - 0.00821(6 - A)^2$$

$$a_1 = 0.5055 - 0.00595(6.5 - A)^2$$

$$k = 0.2711 - 0.01858(2.5 - A)^2$$

The optimal position of the solar receiver is perpendicular on the solar flux direction, like in Fig. 4.

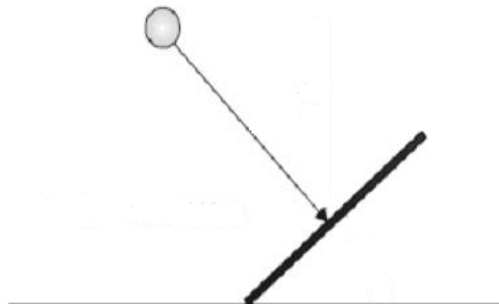


Fig.4. The optimal position of the solar receiver

To completely specify the position of the sun it is three coordinates are needed: the distance between the sun to the Earth, the solar altitude α and the azimuth angle ψ [5]. If one assumes the sun-collector distance from the sun to be constant, the sun position can be specified using two coordinates. The complement of the zenith angle θ_z is the solar altitude α and represents the angle between the horizon and the incident solar beam in a plane

determined by the zenith and the sun. The azimuth angle ψ , is the angular deviation of the sun from directly south (or north in some papers). The azimuth angle is zero at solar noon and increase toward the east. If the azimuth is referenced to north, the solar noon appears at $\psi = 180^\circ$. The hour angle ω is the difference between noon and the desired time. We assume 360° rotation in 24 hours:

$$\omega = \frac{12 - T}{24} \cdot 360^\circ = 15(12 - T)^\circ \quad (5)$$

The all angles used in the sun position determination are shown in the Fig.5.

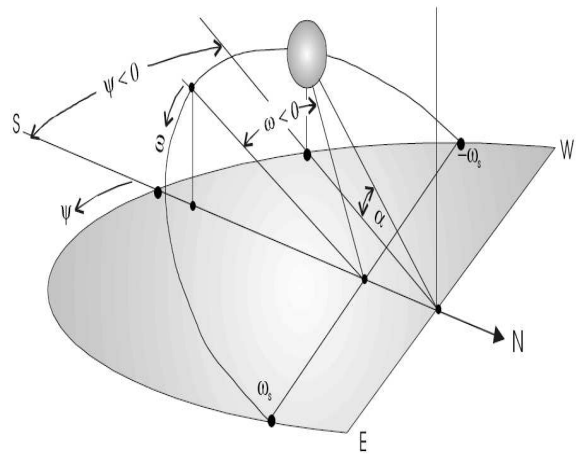


Fig.5. The angles used in sun position determination

If the collecting surface rests in a fixed position, the irradiance must be integrated over daylight hours, taking into account the terms depending on the position. The plots of the solar altitude vs. angular azimuth at the latitude of 35 N, for different month of the year are shown in the Fig.6 [5]

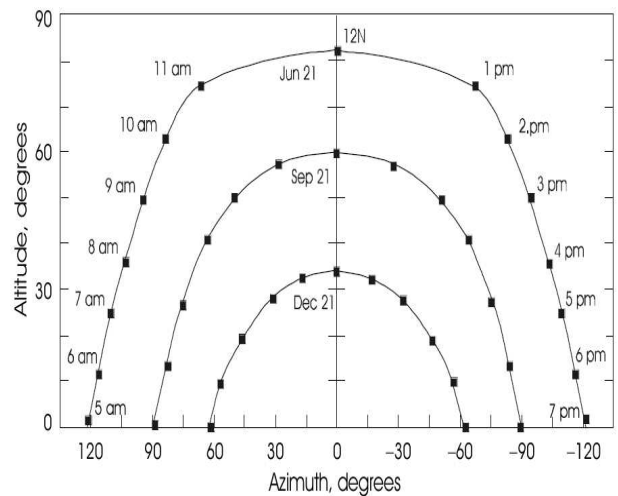


Fig.6. The plots solar altitude vs. azimuth angle

By these reasons, a collecting surface receives different energies from the sun, in accord with the position sun-surface. For a fixed surface, an adjusted one

or a tracking surface, the collected energy is depicted in Fig.7.

The optimized sun energy collecting surface must use a tracking system[6].

The MPPT maximizes the output electrical energy of the photovoltaic (PV) panels.

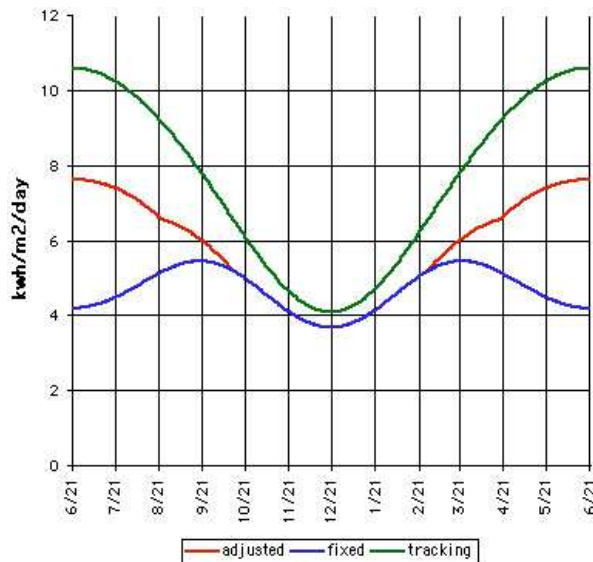


Fig.7. The collected sun energy

2. Tracking control systems

The solar receivers can be mounted either on fixed supports or on mobile supports. Fig.8 shows the additional irradiance received by a tracking collector. In the summer and in a dry climate, approximately 50% more energy can be collected. During the wintertime, only 20% more energy is collected using a tracking system.

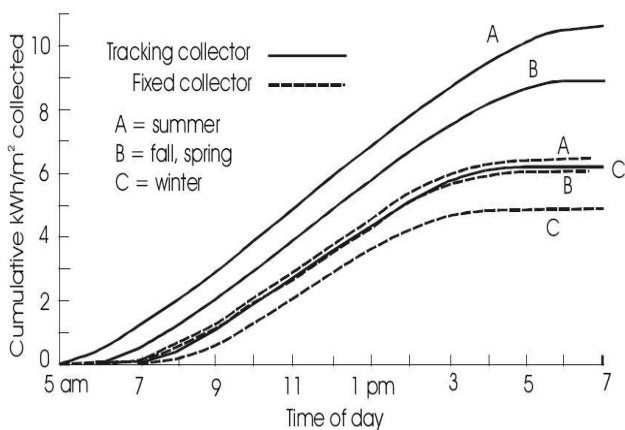


Fig.8. The additional irradiance

One can consider more interesting a single-ax tracking system which rotates about an axis fixed with respect to θ_z . A classical tracking system is a two axis tracking collector(N-S, E-V).

That system uses two important strategies:

-the sensorless control: the plots of the solar altitude vs angular azimuth (see Fig.7) calculated for each time of the day for a given geographical position of the solar collector are computed and stored in a data base. The tracking system controls the position of the collector in accordance with the date and the time.

-the sensor control: the sun position can be specified using two coordinates and the tracking system uses information about these

The standard sensor solution uses two sensors with the structure presented in Fig. 9.

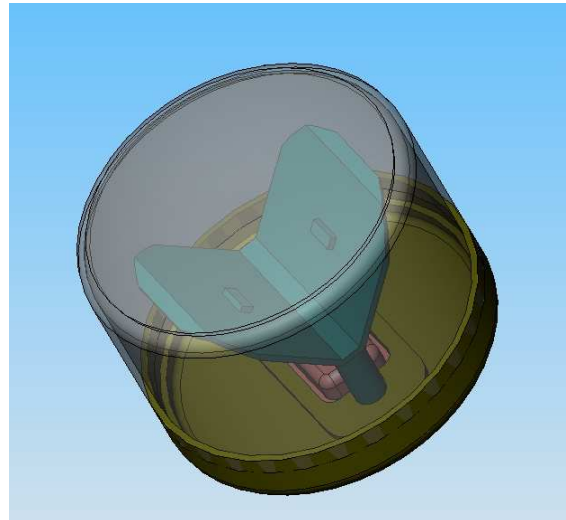


Fig.9. The standard solar sensor

Each sensor is composed by two photo-elements positioned at an angle of 90^0 . The photo-elements are connected in a differential circuit. If the sun collector position is the optimal, the output of the differential circuit is zero. If the sun collector is not in an optimal position with respect to the pair of coordinates, the output of the differential circuit is non zero. The moving on the East-West or South-North directions is driven by the output of the differential circuit.

This solution uses a standard measurement electronic circuit making it susceptible to errors, especially to ageing errors. If the characteristics of the photo-elements change in time, false readings can be made and the optimal collector position is not realized.

3. The new matrix sensor solution

The typical problems of the standard sensor can be solved by the new matrix sensor (MS)solution. The model of the MS is the antique solar clock. Fig.10. shows the initial structure. The MS uses a matrix structure made of photoelements and a cylinder. The location of the cylinder is in a centre of the matrix area. If the position of the solar collector is not optimal, the shadow of the cylinder covers one or more photoelements.

In the optimal position the shadow of the cylinder is minimum and the shadow can not cover the photoelements from the matrix area.

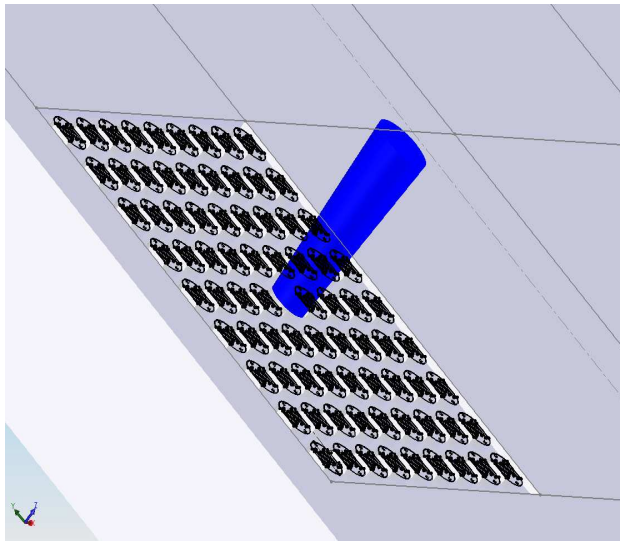


Fig.10. The matrix sensor concept

Several types of photo elements can be used with this matrix sensor topology. The reasoning behind of adoption of the photo resistors (Light Depend Resistor, CdS cell) is explained below. A photoresistor is made of a high resistance semiconductor whose resistance decrease with increasing incident light intensity and the Fig. 11 shows a photoresistor.

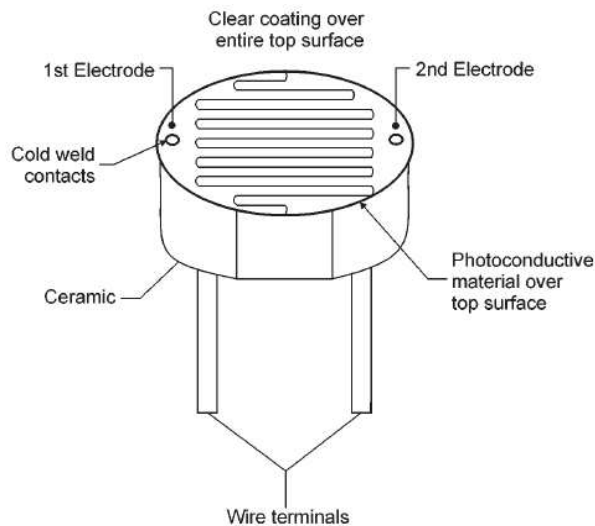


Fig.11. The photoresistor (CdS cell)

The electronic circuit of the photoresistor (a potential divider circuit) is simple, robust and low-cost. There are two possibilities to design the circuit:

- the output voltage increases when the irradiance increases (see Fig.12-a)
- the output voltage decreases when the irradiance increases (see Fig.12-b)

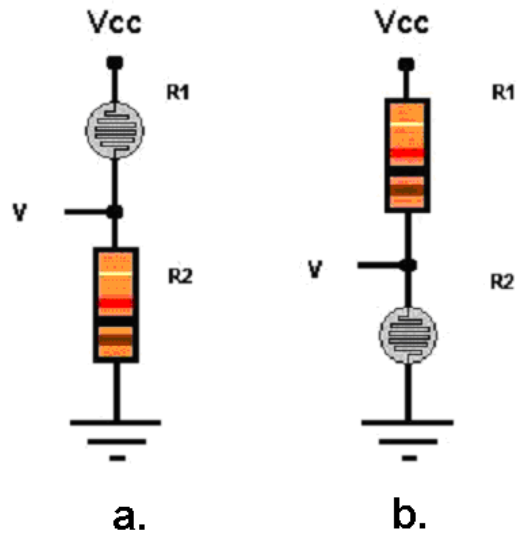


Fig.12. The placement of the photoresistor

For the first circuit (Fig.12.a) the output voltage is:

$$V_{out} = \frac{R_2}{R_2 + R_1} \cdot V_{cc} \quad (6)$$

For the second circuit (Fig.12.b) the output voltage is:

$$V_{out} = \frac{R_1}{R_2 + R_1} \cdot V_{cc} \quad (7)$$

The value of R_1 depends on the level of illumination and in this way, the output voltage estimates the highest irradiance and also the optimal position of the solar collector.

When the solar collector is in the optimal position, all photoresistors are in the lighted area(experience no shading). When the solar collector is not in the optimal position, some of the photoresistors are in the shaded area. Thus, the output voltages of the photoresistors circuits gives the optimal position of the solar collector.

The initial topology of the matrix solar sensor uses a great number of photoresistors (24 sensors). The reason was to obtain information about on optimal position deviation size and the direction of the deviation.

A robust, simple and low-cost sensor demands a new design. The minimized solution is in a Fig.13. This solution uses only eight photoresistors. They are circular mounted around the cylinder.

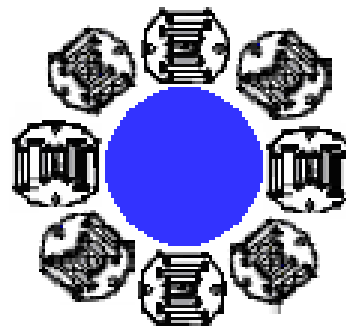


Fig.13. The new matrix sensor topology

Using this new topology, the photoresistors (one, maximum two) from the shaded indicate the direction of movement of the solar collector. In accordance with Fig.14:

-if the photoresistor of the N direction is shadowed, the solar collector must be moved in the S direction

- if the photoresistor of the SV direction is shadowed, the solar collector must be moved in the N direction and E direction

For an increased sensitivity the placement of the photoresistors is made like in Fig.13 and Fig.14. Measured data indicates that the variation of the value R_1 with respect to the light intensity increases.

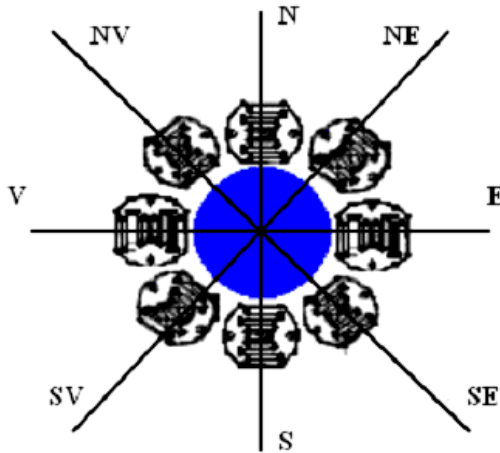


Fig.14. The sensor topology and the movement directions of the solar collector

An important element is the sensor accuracy. The new topology, with eight photoresistors signals the direction of the position corrections. Correct dimensioning of the central cylinder improves the accuracy of the sensor. If the imposed accuracy is 1° , the cylinder height is chosen from the Fig. 14, where:

h = cylinder height

s = shadow dimension

α =the angle between the sun direction and the axe of the cylinder

For a deviation of 1° , the shade of the cylinder covers entirely the photoresistor ($s=8\text{mm}$)

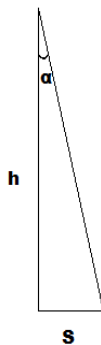


Fig.15. Cylinder height dimensioning

Using these observations, the cylinder height is:

$$h = \frac{s}{\text{tg} \alpha} = \frac{8}{\text{tg} 1^\circ} \approx 46 \text{ [mm]} \quad (8)$$

The next step of the sensor design is to measure all photoresistors for different levels of shadowing. Tab.1. gives the values of photoresistors resistances with respect to the level of illumination. When the photoresistors are completed in the shadow area (0% illumination), the value of the resistance is greater. The resistance are in term of Ω .

Tab. 1. Variation of resistance with respect to the illuminated area of the photoresistor

| | PR1 | PR2 | PR3 | PR4 | PR5 | PR 6 | PR 7 | PR 8 |
|------|-------|-------|-------|-------|-------|-------|-------|-------|
| 100% | 46.4 | 40.6 | 42.8 | 41.4 | 39.4 | 40.4 | 41.8 | 42 |
| 75% | 62.8 | 55 | 61.6 | 54.6 | 50.2 | 53 | 57.4 | 56.6 |
| 50% | 78.4 | 78.2 | 77 | 65.6 | 67.4 | 70.2 | 73.4 | 80.6 |
| 25% | 110.4 | 101.8 | 116.6 | 99.4 | 110.6 | 112.2 | 112.6 | 110 |
| 0% | 263 | 171.2 | 205.2 | 186.6 | 234.2 | 254 | 293 | 307.6 |

Measured data from Tab.1. is used to compute the value of the supplementary resistance R_2 from the Fig. 12.:

$$R_2 = \sqrt{R_{1\text{dark}} \cdot R_{1\text{bright}}} \quad (9)$$

The values of R_2 are calculated using (9) in Tab.2.

Tab. 2. The values of R_2

| | PR1 | PR2 | PR3 | PR4 | PR5 | PR 6 | PR 7 | PR 8 |
|-------|--------|-------|-------|-------|-------|--------|--------|--------|
| R_2 | 110.46 | 83.37 | 93.71 | 87.89 | 96.06 | 101.29 | 110.66 | 113.66 |

The standardized value of R_2 is 120Ω .

Photoresistors of the same type are differ with respect to their individual characteristics (they are not individually measured for their likeness). This is the main reason for the difference between the mounted sensors. Reading errors caused by the use of different sensors with respect to illuminated is depicted in Tab. 3.

Tab.3. Reading errors of photo sensitive resistors for different degrees of illumination (related to the average value)

| | $\varepsilon\%1$ | $\varepsilon\%2$ | $\varepsilon\%3$ | $\varepsilon\%4$ | $\varepsilon\%5$ | $\varepsilon\%6$ | $\varepsilon\%7$ | $\varepsilon\%8$ |
|------|------------------|------------------|------------------|------------------|------------------|------------------|------------------|------------------|
| 100% | 10.9 | -2.9 | 2.3 | 1.1 | -5.8 | -3.4 | -0.1 | 0.4 |
| 75% | 11.3 | -2.5 | 9.2 | -3.2 | -11 | -6 | 1.8 | 0.3 |
| 50% | 6.1 | 5.8 | 4.2 | -11.2 | -8.8 | -5 | -0.7 | 9 |
| 25% | 1.1 | -6.8 | 6.8 | -8.9 | 1.3 | 2.7 | 3.4 | 0.7 |
| 0% | 9.9 | -28.5 | -14.2 | -22 | -2.1 | 6.1 | 22.4 | 28.5 |

Using R_2 (having a standardised value) from the potential divider the output voltage of each photoresistor is obtained. (See Tab.4)

Tab. 4. Output voltages for the 8 photoresistors for different irradiances

| | U1 | U2 | U3 | U4 | U5 | U6 | U7 | U8 |
|------|------|------|------|------|------|------|------|------|
| 100% | 3.60 | 3.73 | 3.68 | 3.71 | 3.78 | 3.74 | 3.70 | 3.71 |
| 75% | 3.28 | 3.42 | 3.30 | 3.43 | 3.52 | 3.46 | 3.38 | 3.39 |
| 50% | 3.02 | 3.02 | 3.04 | 3.23 | 3.20 | 3.15 | 3.10 | 2.99 |
| 25% | 2.60 | 2.70 | 2.53 | 2.73 | 2.60 | 2.58 | 2.57 | 2.60 |
| 0% | 1.56 | 2.06 | 1.84 | 1.95 | 1.69 | 1.60 | 1.45 | 1.40 |

It can be observed that by using R_2 (chosen by the average value of the 8 photo resistors), the reading error is significantly reduced. The error is individually calculated for every shading level with respect to the mean value of all 8 circuits.

Tab.5 contains the output voltage error of the circuits vs. the shading factor.

Tab. 5. Error of the sensor circuit output voltage vs. the average value for different irradiances.

| | $\epsilon\%1$ | $\epsilon\%2$ | $\epsilon\%3$ | $\epsilon\%4$ | $\epsilon\%5$ | $\epsilon\%6$ | $\epsilon\%7$ | $\epsilon\%8$ |
|------|---------------|---------------|---------------|---------------|---------------|---------------|---------------|---------------|
| 100% | -2.9 | 0.5 | -0.1 | 0 | 1.9 | 0.8 | -0.2 | 0 |
| 75% | -3.5 | 0.6 | -2.9 | 0.9 | 3.5 | 1.8 | -0.6 | -0.3 |
| 50% | -2.5 | -2.5 | -1.9 | 4.2 | 3.2 | 1.6 | 0 | -3.5 |
| 25% | 0 | 3.8 | -2.7 | 5 | 0 | -0.8 | -1.1 | 0 |
| 0% | -8.2 | 21 | 8.2 | 14.7 | -0.6 | -5.9 | -14 | -17 |

The multiplexing layout of the output signal of the 8 circuits is presented in Fig.16.

Signals from the potential dividers are compared to constant value of 3V. If the read voltage is greater than then 3V, the photo resistor is considered to be entirely illuminated, else it is considered shade. The length of the cylinder gives a precision of 1 deg. Different characteristics of the photo resistors do not influence the precision of measurements. Fig17. shows the matrix sensor and the electronic circuit. The cylinder is not mounted in the picture.

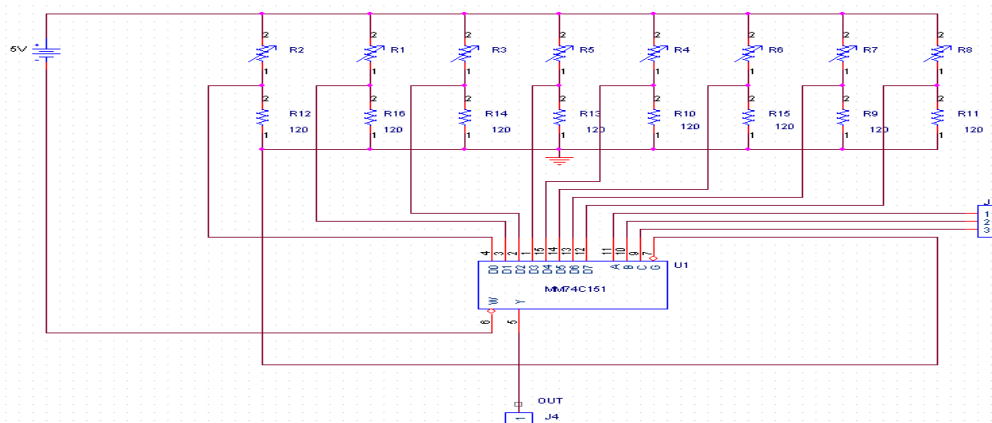


Fig.16. Fotoresistor Signals Multiplexor

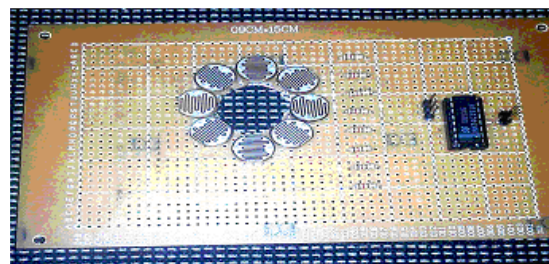


Fig.17. Electronic circuit of the matrix sensor

4. Conclusions

The new matrix solar sensor represents a precise and robust solution for controlling the position of the collector. The expected precision is of 1 deg. The device is immune to errors given by different characteristics of the photo sensors.

The electronic parts used are low cost and easy to mount.

Together with microprocessors or simpler means of control the sensor can be used in a large variety of solar positioning applications.

References

- [1] IPCC-Intergovernmental Panel on Climate Change, Cambridge University Press, 2001
- [2] CMtA-Agricultural Meteorological Report 2006, Romanian Academy Project
- [3] RA Messenger, J Ventre, *Photovoltaic System Engineering*, CRC Press, 2005, sec ed
- [4] A Luque, S hegedus, *Handbook of Photovoltaic Science and Engineering*, Wiley & sons, 2003
- [5] W. Paltz, J. Graf, *European Solar Radiation Atlas*, Sringer, 1996
- [6] JRSof the Commission of the EC, *Guidelines for the Assessment of PV Plans*, Ispra, Italy, 1993